Epidemiological Modelling and Outbreak Prediction using Hyperbolic Geometry

Shreyas Vivek[1], Raghav Pai[2]
The Winchester School

***Abstract*—This paper introduces a novel approach to modeling disease transmission using hyperbolic geometry, specifically the Poincar´e disk model. Traditional models like Susceptible-Infected-Recovered (SIR) assume homogeneous populations, which oversimplifies real-world interactions. By incorporating hyperbolic distance, the Poincar´e disk model captures spatial clustering and irregular social interactions, offering a more realistic framework for studying epidemics. Simulations of the first wave of COVID-19 in India were performed using both the Poincar´e disk and SIR models. Results show that the Poincar´e disk model better captures localized transmission patterns and spatial dynamics, providing deeper insights into how diseases spread through structured populations. This approach highlights the importance of accounting for social network structures in epidemic modeling, offering valuable guidance for targeted public health interventions such as localized lockdowns and vaccination strategies.Our findings demonstrate the advantages of hyperbolic geometry in epidemiological modeling, with potential applications for improving future outbreak predictions and interventions.**

I. INTRODUCTION

The accurate prediction of outbreaks in epidemiology has always been a complex challenge due to the inherent irregularities in population structures and social interactions. Traditional models, such as the Susceptible-Infected-Recovered (SIR) model, have played an important role in understanding epidemic dynamics. However, these models often assume homogeneity across the population, where each individual has an equal probability of interacting with every other individual. In reality, populations are far more complex, with a variety of clustering, network effects, and non-uniform interactions that significantly influence the spread of diseases. This oversimplification can lead to inaccuracies in predicting outbreak patterns, particularly in heterogeneous and densely populated regions.

Hyperbolic geometry offers a powerful alternative for modeling such complex, irregular populations. The Poincar´e disk model, a representation of twodimensional hyperbolic space, is particularly well-suited to address the shortcomings of the traditional models. In hyperbolic geometry, distances between points grow exponentially as one moves away from the center of the disk, capturing the irregular and clustered nature of real-world interactions far more accurately than Euclidean space. This geometry enables the modeling of epidemic spread in a way that accounts for non-uniform population distributions and the varying degrees of connectivity between individuals.

By applying the Poincar´e disk model to epidemic predictions, we can visualize how key nodes and clusters, often representing densely connected populations or highly mobile individuals, serve as epicenters for disease transmission. These nodes can be situated near the center of the disk, representing higher levels of interaction, while more sparsely connected individuals or regions may be located toward the periphery. The hyperbolic distance within the disk captures the exponential increase in infection rates, better simulating the rapid spread of a disease as it moves through these key nodes.

In contrast to the SIR model's assumption of uniform interaction, the Poincar´e disk model introduces a more dynamic and realistic view of epidemic spread. This model not only captures the irregular nature of population interactions but also provides an intuitive visual representation of how disease clusters form and propagate. The inherent structure of the hyperbolic disk allows for more accurate predictions of outbreak intensity, speed, and potential control points for intervention strategies.

This research seeks to develop an outbreak prediction model based on the Poincar´e disk, leveraging hyperbolic geometry to simulate more realistic epidemic spreads. By capturing the non-homogeneous nature of social interactions and understanding how key nodes drive transmission, this model has the potential to enhance current epidemiological predictions and contribute to more effective outbreak management strategies.

II. METRIC SPACES

A metric space is a fundamental concept in mathematics, providing a framework to measure the distance between points in a set. A metric space is formally defined as follows:

Definition 2.1. *A metric space is a set X together with a function $d : X \times X \to \mathbb{R}$, called a metric, that satisfies the following properties for all $x,y,z \in X$:*

1. *Non-negativity: $d(x,y) \geq 0$ and $d(x,y) = 0$ if and only if $x = y$.*
2. *Symmetry: $d(x,y) = d(y,x)$.*
3. *Triangle inequality: $d(x,z) \leq d(x,y) + d(y,z)$.*

The set X is referred to as the underlying set, and d is the distance function or metric.

The concept of a metric space generalizes the idea of distance in Euclidean geometry to more abstract spaces. The distance between points in the metric space does not necessarily need to conform to our intuitive understanding of physical distance but must satisfy the three properties listed above.

Metric spaces allow us to talk about convergence, continuity, compactness, and other topological properties, making them a central object of study in analysis, topology, and geometry.

2.1 Examples of Metric Spaces

1. Euclidean space: The most familiar example of a metric space is $\mathbb{R}^n$, the n-dimensional Euclidean space, with the distance between two points $x = (x_1,x_2,...,x_n)$ and $y = (y_1,y_2,...,y_n)$ given by the Euclidean metric:

$$d(x,y) = \sqrt{(x_1 - y_1)^2 + (x_2 - y_2)^2 + \cdots + (x_n - y_n)^2}.$$

This metric satisfies the non-negativity, symmetry, and triangle inequality properties, making $\mathbb{R}^n$ a metric space.

2. Discrete metric space: Let X be any set, and define the metric $d : X \times X \to \mathbb{R}$ as:

$$d(x,y) = \begin{cases} 0 & \text{if } x = y, \\ 1 & \text{if } x \neq y. \end{cases}$$

This is called the *discrete metric*, and it trivially satisfies the properties of a metric.

3. Hyperbolic geometry: One of the most interesting examples of a metric space arises in hyperbolic geometry. Hyperbolic space is a non-Euclidean space where the geometry differs fundamentally from the Euclidean plane. In this context, the distance between points is measured using a hyperbolic metric, and the space satisfies the properties of a metric space.

Hyperbolic geometry is the study of spaces where the parallel postulate of Euclidean geometry does not hold. One of the most useful models for studying hyperbolic geometry is the *Poincar´e disk model*, which represents hyperbolic space in the unit disk of the complex plane.

The Poincar´e disk model consists of the set:

$$\mathbb{D} = \{z \in \mathbb{C} \mid |z| < 1\},$$

together with a hyperbolic metric that measures distances differently from the Euclidean metric. In the Poincar´e disk model, the distance between two points $z_1,z_2 \in \mathbb{D}$ is defined using the hyperbolic metric:

$$d_{\mathbb{D}}(z_1,z_2) = \operatorname{arcosh}\left(1 + 2\frac{|z_1 - z_2|^2}{(1 - |z_1|^2)(1 - |z_2|^2)}\right).$$

This formula captures the hyperbolic distance, which differs from the Euclidean distance, especially near the boundary of the disk, where distances increase exponentially. As points approach the boundary of the disk, the hyperbolic distance between them tends to infinity, even though the Euclidean distance may remain finite.

III. HYPERBOLIC GEOMETRY

The extension from the comfortable Euclidean plane to a non-Euclidean space is both an attractive and a daunting one. In 1829, Lobachevsky provided the first complete" stable" version of a non-Euclidean geometry, and later mathematicians like Poincar´e developed different models in which these ideas operated. In this paper, we will provide an introduction to the constructs of hyperbolic geometry using two of these models. The first part will be a development of hyperbolic geometry in the plane from an analytic standpoint. We will then use these tools to develop similar ideas in the context of the complex unit disk.

Euclidean geometry is the most prevalent field of geometry, and the one which is most familiar to every student of mathematics. It is based on the five postulates laid down by Euclid in his *Elements*. Given the first four, the last can be paraphrased as follows (2):

" Given a line and a point not on the line, there is at most one line through the point that is parallel to the given line."

Now retain the first four Euclidean postulates, but replace this *parallel postulate* with the following:

" Given a line and a point not on it, there is more than one line going through the given point that is parallel to the given line."

This gives rise to *hyperbolic geometry*.

We begin with the planar construction of hyperbolic geometry and explore what it means to have a curve on the hyperbolic plane:

3.1 Upper Half Plane

Definition 3.1. *The hyperbolic plane is defined to be the upper half of the complex plane:*

$\mathrm{H} = \{z \in \mathrm{C} \mid Im(z) > 0\}$.

Definition 3.2. *A hyperbolic line is the intersection with* H *of a Euclidean circle centered on the real axis or a Euclidean line perpendicular to the real axis in* C *(the extended complex plane* $\mathrm{C} \cup \{\infty\}$*).*

Recall that in the extended complex plane, a line is just the stereographic projection of a circle on the Riemann sphere that runs through the north pole and thus is simply another form of a circle.

Definition 3.3. *Two hyperbolic lines are parallel if they are disjoint.*

The following result introduces a major difference between Euclidean and hyperbolic geometry:

Theorem 3.1. *Let l be a hyperbolic line in* H *and let p be a point in* H *not on l. Then there exist infinitely many distinct hyperbolic lines through p that are parallel to l.*

This contrasts with the Euclidean result, where only one such line exists.

3.2 M¨obius Transformations

Definition 3.4. *A function* $f : \mathrm{C} \to \mathrm{C}$ *is a M¨obius transformation if it is of the form:*

$$f(z) = \frac{az + b}{cz + d}$$

for $a,b,c,d \in \mathrm{C}$ *with* $ad - bc \neq 0$.

It is clear that M¨obius transformations are homeomorphisms since they are compositions of translations, dilations, and inversions, which are all homeomorphisms. Some useful properties of M¨obius transformations are essential for developing the hyperbolic metric.

Theorem 3.2. *M¨obius transformations map circles in the extended complex plane to circles in the extended complex plane.*

Proof. We consider only the case of circles that do not pass through infinity (Euclidean circles) since the other case is similar and easier. Dilations and translations map circles to circles, so we only need to show that the same is true for inversions (functions of the form $w = \frac{1}{z}$). Such a circle is of the form $|z - a|^2 = r^2$, so under the inversion this becomes:

$0 = |1 - aw|^2 - r^2|w|^2$.

Depending on whether $r = |a|$, this equation represents either a line or a circle, both of which are circles in the extended complex plane. □

3.3 Hyperbolic Metric in the Plane

We now apply our knowledge of M¨obius transformations to analyze the geometry of H. First, we define the concept of arc length.

Definition 3.5. *Given a continuous, nonzero function ρ on* R^k*, the length of a piecewise-smooth path* $f : [a,b] \to \mathrm{R}^k$ *is defined as:*

$$length^{\rho}(f) = \int_a^b \rho(f(t))|f'(t)|dt.$$

Definition 3.6. *Given a continuous nonzero function ρ on* H*, we say that length is invariant under M¨ob*(H) *if for any piecewise smooth path* $f : [a,b] \to \mathrm{H}$ *and any* $\gamma \in M¨ob(\mathrm{H})$*, we have:*

$length_\rho(f) = length_\rho(f \circ \gamma)$.

Theorem 3.3. *For every positive constant c, the element of arc length*

$$\rho(z) = \frac{c}{Im(z)}|dz|$$

on H *is invariant under M¨ob*(H).

This leads us to the definition of hyperbolic length in H:

Definition 3.7. *For a piecewise-smooth path* $f : [a,b] \to \mathrm{H}$*, the hyperbolic length of f is defined as:*

$$length^{\mathbb{H}}(f) = \int_a^b \frac{1}{Im(f(t))}|f'(t)|dt.$$

IV. THE POINCAR´E DISC MODEL AND METRIC

We now use the tools developed in the hyperbolic plane to construct the Poincar´e disc model of hyperbolic geometry, operating inside the complex unit disc:

$$D = \{z \in C \mid |z| < 1\}.$$

Theorem 4.1. *All elements of M¨ob*(D) *are of the form:*

$$m(z) = e^{i\theta}\frac{z+a}{1+\overline{a}z}$$

where $\theta \in R$ *and* $a \in \partial D$.

Definition 4.1. *Given a M¨obius transformation* $m : D \to H$, *a hyperbolic line in* D *is the image under* m^{-1} *of a hyperbolic line in* H.

Definition 4.2. *The hyperbolic length of a piecewise-smooth path* $f : [a,b] \to D$ *is defined to be: length*$D(f) = length H(\zeta \circ f)$,

where ζ *is a M¨obius transformation taking* D *to* H.

The Poincar´e disk model is a two-dimensional space for hyperbolic geometry.

All points are contained within the unit disk. Formally, this can be denoted as

$D = \{x \in R^2 \mid |x| < 1\}$

Points in the Poincar´e disk model correspond to points inside the open unit disk. The geodesic i.e. 'straight line' in this hyperbolic space can be represented as the intersection of the unit disk with the Euclidean circles which are orthogonal to its boundary. In other words, it is the arc of a circle that intersects the unit disk at right angles. Note that if the two points are co-linear with respect to the origin, the geodesic is just the straight line passing through the center of the disk.

4.1 Distances in the Poincar´e disk

The disc model of hyperbolic space, denoted D, consists of the unit disc in the complex plane. This is represented by the set:

$$D = \{z = x + iy \mid \sqrt{x^2 + y^2} < 1\}.$$

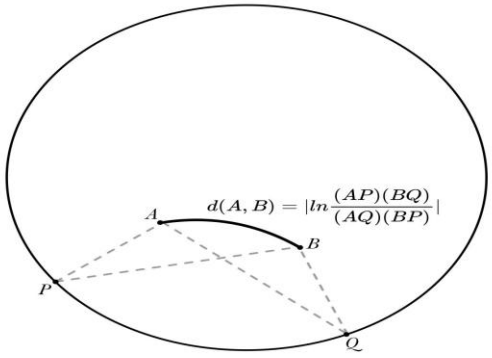

Figure 1: Distances in the Poincar´e disk

The metric of D is given by:

$$ds^2 = \frac{4(dx^2+dy^2)}{(1-x^2-y^2)^2} = \frac{dzd\overline{z}}{(1-|z|^2)^2}.$$

This metric describes distances in the hyperbolic geometry of the unit disc.

We can compute the distance between two points A and B in the Poincar´e disk as follows :

$$d(A,B) = |ln\frac{(AP)(BQ)}{(AQ)(BP)}|$$

Where P and Q are the ideal endpoints of the Poincar´e line determined by A and B, and the distances *AP*, *BQ* etc. are the conventional Euclidean straight line distances.

Let $z_1, z_2 \in D$ be two points in the Poincar´e disk. The hyperbolic geodesic between z_1 and z_2 is given by the unique circular arc that passes through both points and is orthogonal to the boundary of the disk. If the points are on a line passing through the center of the disk, the geodesic is a straight line. The hyperbolic distance between two points $z_1, z_2 \in D$ in the Poincar´e disk is given by the formula:

$$d_D(z_1,z_2) = \text{arcosh}\left(1 + 2\frac{|z_1 - z_2|^2}{(1-|z_1|^2)(1-|z_2|^2)}\right).$$

V. HYPERBOLIC GEODESICS

In hyperbolic geometry, a *geodesic* is the shortest path between two points, analogous to a straight line in Euclidean geometry. In the hyperbolic plane, geodesics differ from Euclidean straight lines and are represented by curves that depend on the chosen model of hyperbolic geometry. One of the most commonly used models is the *Poincar´e disk model*, where hyperbolic geodesics are circular arcs.

Geodesics in the Poincar´e Disk Model

In the Poincar´e disk model, the hyperbolic plane is represented by the unit disc:

$D = \{z \in C \mid |z| < 1\}$.

In this model, the geodesics are either:

- Circular arcs that are perpendicular to the boundary of the unit disk.
- Euclidean diameters of the unit disk.

These geodesics minimize the hyperbolic distance between two points inside the disk.

Geodesics in the Upper-Half Plane Model

The geodesics of Hare lines perpendicular to the real line, and half-circles orthogonal to the real line.

5.1 Properties of Hyperbolic Geodesics

Hyperbolic geodesics have several important properties:

- They are invariant under M¨obius transformations that preserve the disk.
- Geodesics are the unique shortest paths between two points in the hyperbolic plane.
- As points approach the boundary of the disk, the hyperbolic distance between them grows exponentially, even though their Euclidean distance may remain small.

Theorem 5.1. *For any two distinct points z_0,z_1 in* D*, there is a unique shortest curve in* D *from z_0 to z_1 in the hyperbolic metric, namely, the arc of the circle passing through z_0 and z_1 that is orthogonal to the unit circle.*

Definition 5.1. *The described paths in Theorem 5.1 are called hyperbolic geodesics.*

Theorem 5.2. *The hyperbolic distance from* 0 *to z is given by the formula:*

$$d(0,z) = \log\left(\frac{1+|z|}{1-|z|}\right).$$

In hyperbolic geometry, the shortest paths between two points, known as *geodesics*, are represented by circular arcs that are perpendicular to the boundary of the disk. These geodesics differ significantly from Euclidean straight lines, reflecting the curved nature of hyperbolic space.

The geodesic between two points z_1,$z_2 \in$ D can be visualized as an arc of a circle that intersects the boundary of the disk at right angles. The hyperbolic distance between the two points along this arc is given by the hyperbolic metric.

VI. THE SIR MODEL: AN EXISTING OUTBREAK PREDICTION MODEL

The Susceptible-Infected-Recovered (SIR) model is a classic compartmental model used in epidemiology to describe the spread of infectious diseases in a population. The model divides the population into three compartments:

- $S(t)$: The number of susceptible individuals at time t, who are at risk of contracting the disease.
- $I(t)$: The number of infected individuals at time t, who are currently capable of spreading the disease to susceptible individuals.
- $R(t)$: The number of recovered individuals at time t, who have either recovered from the disease and gained immunity or have been removed from the susceptible population (through recovery, isolation, or death).

The SIR model tracks the transition of individuals between these compartments over time based on the disease's transmission and recovery rates.

6.1 SIR Model Differential Equations

The SIR model is governed by a set of three ordinary differential equations (ODEs) that describe the rate of change of each compartment over time. These equations are:

$$\frac{dS}{dt} = -\beta S(t)I(t)$$

$$\frac{dI}{dt} = \beta S(t)I(t) - \gamma I(t)$$

$$\frac{dR}{dt} = \gamma I(t)$$

Where:

- β is the transmission rate or infection rate, which represents the rate at which susceptible individuals come into contact with infected individuals and contract the disease.
- γ is the recovery rate, which represents the rate at which infected individuals recover from the disease and move to the recovered compartment.

6.2 Explanation of Each Equation

1. Susceptible Compartment ($S(t)$)

The first differential equation describes the rate of change of the number of susceptible individuals:

$$\frac{dS}{dt} = -\beta S(t)I(t)$$

This equation indicates that the susceptible population decreases over time as individuals become infected. The rate at which susceptible individuals are removed from the $S(t)$ compartment depends on the product of $S(t)$ and $I(t)$, which reflects the number of contacts between susceptible and infected individuals. The factor β scales this product to represent the probability of disease transmission per contact.

The negative sign reflects that the number of susceptible individuals decreases as they transition to the infected compartment.

2. Infected Compartment ($I(t)$)

The second differential equation governs the number of infected individuals:

$$\frac{dI}{dt} = \beta S(t)I(t) - \gamma I(t)$$

The number of infected individuals increases when susceptible individuals contract the disease, which is captured by the term $\beta S(t)I(t)$. At the same time,

infected individuals either recover or are removed from the population, and this is represented by the term $\gamma I(t)$, which decreases the number of infected individuals.

Thus, the overall change in the infected population is the difference between the number of newly infected individuals and the number of individuals recovering or being removed.

3. Recovered Compartment ($R(t)$)

The third differential equation describes the dynamics of the recovered population:

$$\frac{dR}{dt} = \gamma I(t)$$

This equation states that the recovered population increases at a rate proportional to the number of infected individuals, as infected individuals recover or are removed from the infectious pool at the rate γ. The recovered individuals are assumed to gain immunity to the disease or be removed from the susceptible population (e.g., through isolation or death).

6.3 Basic Reproduction Number (R_0)

A key parameter in the SIR model is the basic reproduction number, denoted R_0, which is defined as the expected number of secondary infections caused by a single infected individual in a fully susceptible population. It is given by the ratio of the transmission rate to the recovery rate:

$$R_0 = \frac{\beta}{\gamma}$$

The value of R_0 determines the behavior of the epidemic:

- If $R_0 > 1$, the disease will spread and potentially cause an epidemic, as each infected individual is, on average, infecting more than one other person.
- If $R_0 < 1$, the disease will die out, as each infected individual infects fewer than one person on average, leading to a decrease in the number of infected individuals.

6.4 Interpretation of the SIR Model

The SIR model is useful for understanding the dynamics of disease outbreaks and for predicting how the epidemic will evolve over time. The model can predict when the peak of the infection will occur, how long the epidemic will last, and what proportion of the population will eventually be infected.

At the start of an epidemic, the number of susceptible individuals is large, and the infection spreads rapidly. As more people become infected, the number of susceptible individuals decreases, which eventually slows down the rate of infection. The epidemic reaches its peak when the number of newly infected individuals starts to decline, which occurs when the susceptible population has decreased to a level where each infected individual is no longer infecting more than one other person (i.e., when R_0 approaches 1).

Eventually, the epidemic dies out as the number of susceptible individuals decreases, and the population transitions to the recovered state. The number of infected individuals approaches zero, and the disease no longer spreads.

6.5 Limitations of the SIR Model

While the SIR model provides valuable insights into disease dynamics, it has several limitations:

- The model assumes that the population is well-mixed, meaning that every individual has an equal probability of interacting with every other individual. This is not always realistic, especially in structured populations where interactions are more localized.
- The model assumes permanent immunity after recovery, which may not be the case for all diseases. For diseases with temporary immunity or recurrent infections, a more complex model (such as the SIRS model) may be required.
- The SIR model does not account for factors such as birth, death, or migration, which can alter the dynamics of the population and the spread of the disease.

The SIR model is a simple but powerful tool for understanding the spread of infectious diseases in a population. Its differential equations provide a framework for predicting the dynamics of an epidemic, including how quickly the disease will spread, when the epidemic will peak, and how many individuals will eventually be infected. Despite its limitations, the SIR model remains a foundational model in epidemiology, and more complex models can build on its framework to address real-world complexities such as spatial structure, heterogeneous mixing, and temporary immunity.

VII. POINCARE DISC MODEL DESCRIPTION

This model considers the spread of a disease in a population where individuals (or nodes) are represented in the Poincar´e disk. The Poincar´e disk is a model of hyperbolic geometry where points inside the unit disk represent nodes, and the distance between

any two nodes is calculated using the hyperbolic distance formula.

Modeling the Probability of Disease Transmission

The probability of disease transmission between two nodes, A and B, is modeled using an exponential function that depends on the hyperbolic distance $d(A,B)$ between them. This distance is calculated using the Poincar´e distance formula:

$$d(A,B) = \operatorname{arcosh}\left(1 + 2\frac{|A-B|^2}{(1-|A|^2)(1-|B|^2)}\right).$$

The probability function is given by:

$$p(A,B) = \frac{1}{1+e^{\alpha(d-\beta)}}$$

where:

- d is the Poincar´e distance between nodes A and B,
- α controls the steepness of the transition,
- β represents the threshold distance where the probability starts increasing significantly.

This model captures the idea that individuals closer to each other in the hyperbolic space have a higher probability of transmitting the disease, while those further apart have a lower probability. The hyperbolic metric models the exponential growth in transmission potential that characterizes real-world epidemics, especially in densely connected clusters.

Parameters and Their Interpretation

Parameter α

The parameter α governs how quickly the probability transitions from low to high as the distance between two nodes decreases. A larger value of α means that the probability of transmission sharply increases over a small change in distance. This could represent highly contagious diseases that spread even with minimal contact.

Parameter β

The threshold parameter β shifts the curve along the distance axis, determining the distance at which transmission becomes more likely. A smaller β would imply that even distant nodes have a higher probability of transmitting the disease, while a larger β implies that transmission is only likely at very close distances.

To estimate these parameters, we apply *maximum likelihood estimation* (MLE) techniques, using observed transmission data to determine the values of α and β that maximize the likelihood of the observed transmission events.

Transmission Dynamics and Hyperbolic Geometry

Using the Poincar´e disk as a geometric representation of the population allows us to model disease transmission in a way that accounts for the clustered and irregular nature of human interactions. In hyperbolic space:

- Clusters of individuals (or nodes) near the center of the disk are more likely to be densely connected, resulting in a higher probability of disease transmission within these clusters.
- Peripheral nodes (closer to the boundary of the disk) represent individuals or regions that are more isolated, with lower probabilities of disease transmission due to larger hyperbolic distances between them and other nodes.

Outbreak Prediction

The probability function $p(A,B)$ plays a central role in predicting outbreaks. By calculating the transmission probability between every pair of nodes in the Poincar´e disk, we can simulate the spread of the disease across the population.

The model allows us to predict how quickly and widely the disease will spread based on:

- Initial conditions: The location of infected individuals in the Poincar´e disk.
- Population structure: How nodes are distributed across the disk, with more densely connected nodes closer to the center.
- Transmission probability: Governed by the parameters α and β, which determine how likely the disease is to spread given the distance between individuals.

By running simulations of the disease transmission, we can predict: • The likely epicenters of the outbreak, typically represented by clusters of individuals near the center of the Poincar´e disk.

- The rate at which the disease spreads to peripheral regions, which are less densely connected. • The overall trajectory of the outbreak, including the expected number of infections over time.

Estimating Parameters Using Maximum Likelihood

To estimate the values of α and β, we collect data on disease transmission between pairs of individuals (nodes). For each pair, we observe whether transmission occurred (binary outcome: 1 if transmitted, 0 otherwise), along with the corresponding Poincar´e distance d between them.

The likelihood function for the observed data is given by:

$$L(\alpha,\beta) = \prod_{i=1}^{n} p(A_i,B_i)^{y_i}\,(1-p(A_i,B_i))^{1-y_i}$$

where:

- $p(A_i,B_i)$ is the transmission probability between the i-th pair of nodes,
- y_i is the observed outcome (1 if transmission occurred, 0 if not),
- n is the total number of observed pairs.

By maximizing this likelihood function, we estimate the parameters α and β, which provide a calibrated model that best fits the observed transmission data.

Applications and Real-World Implications

This outbreak prediction model offers several advantages over traditional models like the SIR (Susceptible, Infected, Recovered) model: • It accounts for the irregular and clustered nature of human interactions by representing individuals in hyperbolic space.

- It uses hyperbolic distance to reflect the exponential growth in transmission risk for densely connected individuals or groups.
- It provides a more nuanced view of transmission dynamics, particularly in populations that are not uniformly mixed.

By accurately modeling the probability of disease transmission and predicting the trajectory of outbreaks, this model can inform public health interventions, such as targeted vaccination or quarantine measures, aimed at reducing the spread of the disease.

VIII. RESULTS OF THE POINCARE DISC MODEL

Transmission Probability vs. Hyperbolic Distance

The test was conducted over 18-time steps, representing the 18 weeks of the first wave of COVID-19 in India, from August 31st, 2020, to January 1st, 2021. The initial data was based on the number of infected individuals per 1,000 Indians. The simulation utilized 1000 random points representing individuals on the Poincar´e disk.The graphs (2, 3, 4) depict how the probability of disease transmission changes as a function of hyperbolic distance between two nodes (representing individuals) on the Poincar´e disk. These graphs were generated for different weeks of the simulation, each representing a different stage in the spread of the disease over time: Week 1, Week 9, and Week 18.

The transmission probability decreases exponentially as the hyperbolic distance between two individuals increases. This relationship is intuitive, as individuals further apart in hyperbolic space have a lower chance of transmitting the disease. Hyperbolic distance reflects the clustering and density of interactions, providing a more realistic model than Euclidean distance.

- In Week 1, when the number of infected individuals is relatively small, the transmission probability is high for small hyperbolic distances (close proximity). The probability rapidly decays as the hyperbolic distance increases.
- By Week 9, more individuals have been infected. The probability curve shifts slightly, showing that the spread of the disease reaches slightly further distances, even though the probability at larger distances remains low.
- By Week 18 the infection is widespread, and the transmission probability curve has flattened further. The probability at small distances is still significant, but the decay is more gradual compared to Week 1.

These results suggest that as more individuals become infected, the disease spreads to a greater extent across the population. Initially, the outbreak is localized, but over time, the transmission probability at slightly larger hyperbolic distances increases.

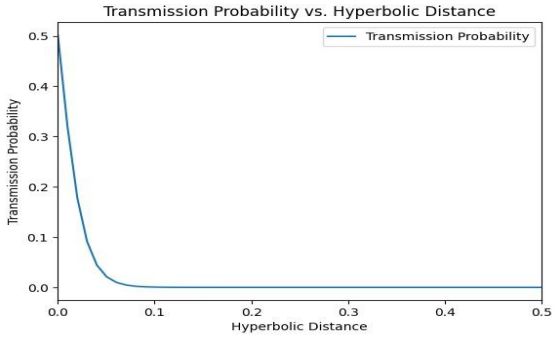

Figure 2: Transmission Probability vs. Hyperbolic Distance (Week 1)

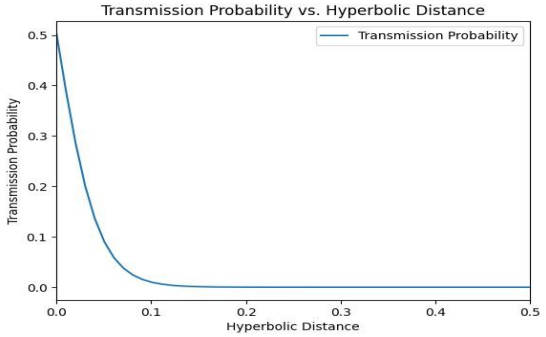

Figure 3: Transmission Probability vs. Hyperbolic Distance (Week 9)

Analysis of α and β Parameters

The estimated average values of the parameters α and β across the 18 weeks are presented in the table. The parameter β remains constant at a low value (0.01), indicating that the baseline transmission probability, i.e., the probability of transmission when the hyperbolic distance is close to zero, does not change

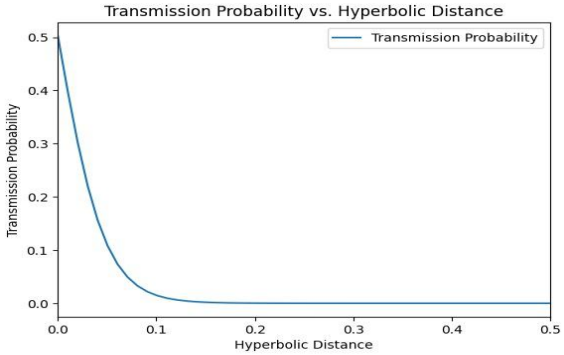

Figure 4: Transmission Probability vs. Hyperbolic Distance (Week 18)

significantly over time. This suggests that the probability of transmission in close proximity remains consistently high throughout the simulation period.

The parameter α, which controls the rate at which transmission probability decays with increasing hyperbolic distance, shows more dynamic behavior:

- In Week 1, α has a high value (over 91.2), indicating a rapid decay of transmission probability with increasing hyperbolic distance. This means that in the early stages of the outbreak, the disease spreads mainly among individuals who are very close in terms of hyperbolic distance (representing close physical or social proximity).
- Over time, α steadily decreases. By Week 18, α has dropped to 42.7, indicating that the decay of transmission probability has slowed significantly. This suggests that as more individuals become infected, the disease spreads more easily over larger distances in hyperbolic space.

This decreasing trend in α indicates that the spread of the disease becomes less localized as the epidemic progresses. Initially, the outbreak is confined to small, tightly connected clusters. However, as more people become infected, the disease reaches individuals who are further apart in terms of hyperbolic distance.

Interpretation of the Results

These results offer valuable insights into the behavior of the disease transmission model:

- Constant β: The constancy of β suggests that the baseline transmission probability (i.e., the probability of transmission at zero hyperbolic distance) is primarily determined by the intrinsic characteristics of the disease, such as its infectiousness. The disease remains highly contagious at close distances throughout the simulation.
- Decreasing α: The gradual decrease in α shows that, as the disease spreads, it becomes easier for the disease to reach individuals who are further apart in hyperbolic space. In the early stages of the epidemic, the spread is confined to local clusters, but as more people become infected, interactions with more distant individuals become more likely.

Week (31/8/2020 - 1/1/2021)	Infected per 10,000	Alpha1	Alpha2	Alpha3	Beta1	Beta2	Beta3	AvgAlpha	AvgBeta
1	25	71.7	89.9	112.1	0.01	0.01	0.01	91.23333333	0.01
2	28	76.4	72.3	78.8	0.01	0.01	0.01	75.83333333	0.01
3	33	59.9	70	67.8	0.01	0.01	0.01	65.9	0.01
4	38	62.5	68.4	63.2	0.01	0.01	0.01	64.7	0.01
5	42	72.9	52.8	79.7	0.01	0.01	0.01	68.46666667	0.01
6	46	60.3	57.1	51.3	0.01	0.01	0.01	56.23333333	0.01
7	49	51.7	50	57.2	0.01	0.01	0.01	52.96666667	0.01
8	52	64.1	54.9	46.2	0.01	0.01	0.01	55.06666667	0.01
9	55	51	49	49	0.01	0.01	0.01	49.66666667	0.01
10	57	49	44.1	47.6	0.01	0.01	0.01	46.9	0.01
11	60	56.6	49.2	48	0.01	0.01	0.01	51.26666667	0.01
12	62	47.4	52.5	60.9	0.01	0.01	0.01	53.6	0.01
13	64	42.3	49.5	39.6	0.01	0.01	0.01	43.8	0.01
14	66	46.7	48.1	42.4	0.01	0.01	0.01	45.73333333	0.01
15	68	37.1	42.3	38.2	0.01	0.01	0.01	39.2	0.01
16	69	40.5	49.3	48	0.01	0.01	0.01	45.93333333	0.01
17	70	38.6	36.2	41	0.01	0.01	0.01	38.6	0.01
18	71	42.7	39.8	45.6	0.01	0.01	0.01	42.7	0.01

Figure 5: Estimated average α and β values

These results have significant implications for public health strategies during an outbreak. Early in the epidemic, when α is high and the disease spreads rapidly within small clusters, targeted interventions such as quarantine measures or localized lockdowns are likely to be effective. Isolating these clusters early

can prevent the disease from spreading to more distant parts of the network.

As the outbreak progresses and α decreases, the disease spreads more widely across the population, and broader interventions are required. Mass testing, widespread vaccination, and social distancing measures are critical at this stage to prevent the disease from reaching new, previously uninfected areas

IX. RESULTS OF THE S-I-R MODEL

The SIR (Susceptible, Infected, Recovered) simulation (6, 7) was conducted over 18 time steps, representing the 18 weeks of the first wave of COVID-19 in India, from August 31st, 2020, to January 1st, 2021. The initial data was based on the number of infected individuals per 1,000 Indians. The simulation utilized 1000 random points representing individuals on the Poincar´e disk. These points were divided into three categories over time: susceptible (blue), infected (orange), and recovered (green).

- The simulation started with 25 randomly selected points initially infected.
- Using the transmission probability function in the Poincar´e disk:

$$p(A, B) = \frac{1}{1 + e^{\alpha(d-\beta)}}$$

the probability of infection was computed based on the hyperbolic distance between individuals.

As time progressed, the simulation tracked how the infection spread through the population. The results can be visualized through two figures: - The first figure (6) shows how the number of susceptible, infected, and recovered individuals changes over time. - The second figure (7) shows the final state of the simulation, where the positions of susceptible, infected, and recovered individuals are mapped onto the Poincar´e disk after 18 weeks.

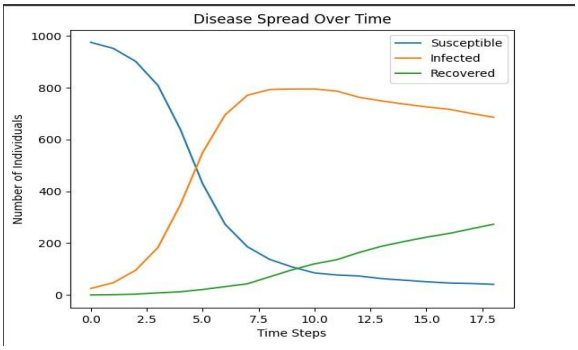

Figure 6: Disease Spread Over Time - SIR Model

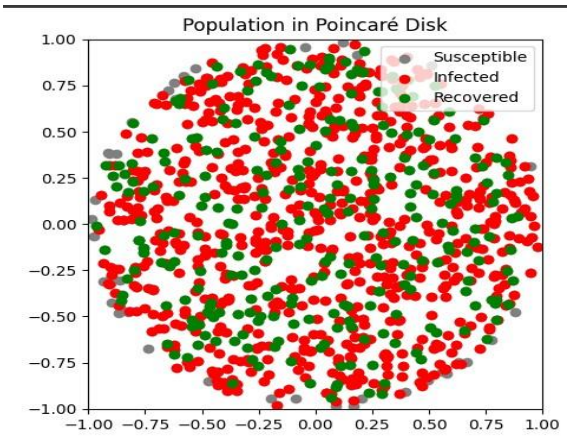

Figure 7: Poincar´e Disk Representation - SIR Model

Analysis of the SIR Model Results

A)Time Evolution of Disease Spread

Figure 6 shows the evolution of the disease spread over 18 time steps: - At the beginning, there is a rapid increase in the number of infected individuals as the disease spreads through the susceptible population. - The number of infected individuals peaks between time steps 5 and 7, with a sharp decline afterward as more individuals recover or are no longer susceptible. - The susceptible population decreases rapidly during the first few weeks, indicating a fast spread of the disease. - The recovered population steadily increases as infected individuals recover, and by the 18th time step, the majority of the population is recovered, with very few susceptible or infected individuals remaining.

B) Poincar´e Disk Representation of Disease Spread

In Figure 7, the final state of the simulation after 18 weeks is mapped onto the Poincar´e disk. The disk shows the spatial distribution of susceptible, infected, and recovered individuals. Key observations include: - The disk is densely populated with recovered individuals (green points), indicating that most of the population has been infected and recovered by the end of the simulation. - Some susceptible individuals (blue points) remain, mainly in regions that are further from the initially infected individuals in terms of hyperbolic distance. - Infected individuals (orange points) are scattered sparsely across the disk, indicating that the infection is in the process of being eradicated.

The Poincar´e disk model effectively captures the spatial clustering of disease transmission, where individuals who are closer in hyperbolic distance have

a higher probability of transmitting the disease to one another.

X. COMPARISON OF S-I-R WITH THE POINCAR´E DISK TRANSMISSION MODEL

While the SIR model provides a simplified representation of disease dynamics with three key compartments (susceptible, infected, and recovered), the Poincar´e disk model introduces a more realistic spatial component to the simulation. The Poincar´e disk model considers not only the number of individuals in each compartment but also their spatial distribution and clustering. The key differences are as follows

1. Spatial Representation: The SIR model does not account for the spatial distribution of individuals, treating them as a homogeneous population where each individual has an equal probability of interacting with every other individual. In contrast, the Poincar´e disk model incorporates hyperbolic distance to account for the spatial clustering of individuals. This clustering is evident in Figure 7, where recovered and infected individuals are spread across the disk based on their proximity in hyperbolic space.
2. Transmission Probability: In the SIR model, the probability of disease transmission is generally constant and does not depend on the spatial distance between individuals. On the other hand, the Poincar´e disk model uses the exponential transmission function $p(A,B)$, which depends on the hyperbolic distance between individuals. This leads to more accurate modeling of disease spread in real-world scenarios where individuals are more likely to transmit the disease to those in close proximity.
3. Clustering Effect: The Poincar´e disk model captures the natural clustering of disease spread, where clusters of infected individuals form around areas with high population density in hyperbolic space. In the SIR model, this effect is not explicitly modeled, leading to a less realistic representation of disease spread in structured populations.
4. Infection Over Time: The SIR model exhibits a rapid initial increase in infections followed by a peak and subsequent decline as individuals recover. This behavior is also observed in the Poincar´e disk model, but the spatial component allows for a more nuanced understanding of how infections spread and decay within different clusters of individuals.

The comparison between the SIR model and the Poincar´e disk model highlights the importance of incorporating spatial and hyperbolic distance factors into disease modeling: - The Poincar´e disk model provides a more realistic representation of how diseases spread in structured populations, where individuals are more likely to interact with those nearby in physical or social space. - By incorporating hyperbolic geometry, the Poincar´e disk model can capture the effects of clustering, which are crucial for understanding the dynamics of real-world epidemics like COVID-19.

XI. CONCLUSION

In this paper, we explored the application of hyperbolic geometry, specifically the Poincar´e disk model, to model disease transmission in populations. By leveraging the unique properties of hyperbolic space, we developed a framework that captures the spatial clustering and irregular interaction patterns inherent in real-world populations, which traditional models like the SIR model often fail to represent accurately.

Our analysis began by modeling the probability of disease transmission between individuals in the Poincar´e disk, where the hyperbolic distance between two nodes (individuals) determines the likelihood of transmission. This approach provided a more dynamic and realistic understanding of how disease spread is influenced by proximity in hyperbolic space, capturing the exponential decay in transmission probability with increasing distance.

The SIR model was then implemented to simulate the first wave of COVID19 in India, illustrating the temporal evolution of susceptible, infected, and recovered individuals over 18 weeks. We observed a rapid rise in infections, followed by a peak and subsequent decline as individuals recovered. The final state of the epidemic was visualized on the Poincar´e disk, where the spatial distribution of individuals across the disk further reinforced the clustering effects.

By comparing the SIR model to the Poincar´e disk model, we highlighted key differences, particularly the impact of incorporating spatial structure into the transmission dynamics. The Poincar´e disk model successfully captured the localized spread of disease within clusters of individuals, offering a more granular

perspective than the homogeneous assumptions of the SIR model. The spatial variation, as modeled by hyperbolic distances, allowed us to analyze how disease spread changes not only over time but also across different regions of the population, represented by their positions on the Poincar´e disk.

The results of the simulations demonstrated that incorporating hyperbolic geometry into epidemiological models provides a more comprehensive understanding of how diseases spread in complex networks. While the SIR model is useful for broad epidemiological trends, the Poincar´e disk model can capture localized behaviors that are essential for planning targeted interventions, such as quarantine measures or localized lockdowns.

In conclusion, our work emphasizes the value of using geometric models to simulate the spread of diseases in structured populations. The Poincar´e disk model provides a robust framework for understanding disease transmission in environments where interactions are not uniformly distributed, paving the way for more accurate predictions of outbreak dynamics and more effective public health strategies. Future work can build on this model by incorporating additional factors, such as movement patterns, mobility restrictions, and vaccination strategies, to further enhance our understanding of epidemic spread in complex social systems.

REFERENCES

[1] Adiga A, Dubhashi D, Lewis B, Marathe M, Venkatramanan S, VullikantiA. Mathematical Models for COVID-19 Pandemic: A Comparative Analysis. J Indian Inst Sci. 2020;100(4):793-807. doi: 10.1007/s41745-02000200-6. Epub 2020 Oct 30. PMID: 33144763; PMCID: PMC7596173.

[2] Thorgeirsson, Sverrir. “Hyperbolic geometry: history, models, and axioms.” U.U.D.M. Project Report, June 2014.

[3] Beltrami, Eugenio. The Poincar´e Disk Model for Hyperbolic Geometry. 1854.

[4] Ghosh, Palash, et al. “COVID-19 in India: Statewise Analysis and Prediction.” JMIR Public Health and Surveillance, vol. 6, no. 3, Aug. 2020, p. e20341. https://doi.org/10.2196/20341.